



An Advanced Controller for Improving the Performance of Single Phase 7-Level Inverter for Grid Connected PV System

M. Murali Krishna, P. Chandra Babu

PG Scholar, Department of Electrical and Electronics Engineering, QIS Institute of Technology, Ongole, A.P, India
Assistant Professor, Department of Electrical and Electronics Engineering, QIS Institute of Technology, Ongole, A.P,
India

ABSTRACT: This paper proposes a fuzzy controller for advancing the performance of a seven level multilevel inverter for grid connected photovoltaic system. This topology gives reduced THD and improved wave shape rather than conventional controlled seven level inverter. Here we are using three identical reference signals (V_{ref1} , V_{ref2} , and V_{ref3}) with offset value same as amplitude of the triangular carrier ($V_{carrier}$) signal to generate the PWM signals. Pv based inverter providing seven levels of output voltage and it recounts the improvement of novel modified H-bridge single phase multilevel inverter, it has two diode bidirectional switches and a novel pulse width modulation technique. By controlling the modulation index, the required number of levels of the inverter's output voltage can be achieved. This topology is advantages in MPPT system. Multilevel inverter with FUZZY control implementation is advantages in improved output waveform, lower the THD and fast error correction. The proposed system was verified through MATLAB/Simulation program.

KEYWORDS: Fuzzy logic, Micro Grid, MPPT, pulse width modulation PWM, photovoltaic (PV) system, and THD.

I. INTRODUCTION

1.1 MULTILEVEL INVERTOR

Multilevel inverter technology has emerged recently as a very important alternative in the area of high-power medium-voltage energy control. The popular methods are diode-clamped inverter (neutral-point clamped), capacitor-clamped (flying capacitor), and cascaded multilevel inverters with separate DC sources. The last one is most fusible topology used in all areas. This paper presents the most relevant structure of the multilevel inverter using cascaded-inverters with separated dc sources will be introduced, as well as switching pattern.

1.1.1 Full-bridge or "H-bridge" Voltage Source Inverter

The smallest number of voltage levels for a multilevel inverter using cascaded-inverter with SDCSs is three. To achieve a three-level waveform, a single full-bridge inverter is employed. Basically, a full-bridge inverter is known as an H-bridge cell, which is illustrated in Fig. 1. The inverter circuit consists of four main switches and four freewheeling diodes.

International Journal of Advanced Research in Electrical, Electronics and Instrumentation Engineering

(An ISO 3297: 2007 Certified Organization)

Vol. 3, Issue 11, November 2014

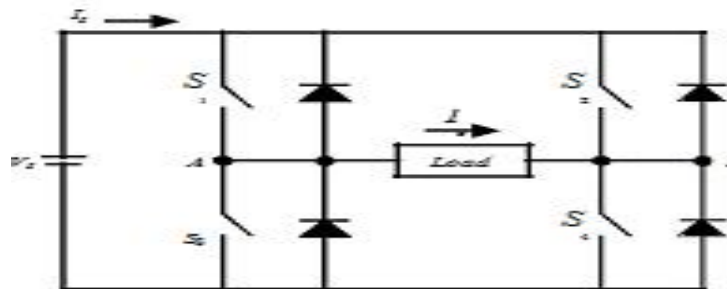


Figure: 1. An H-bridge cell

1.2 CASCADED H-BRIDGES INVERTER

A single-phase structure of an m-level cascaded inverter is illustrated in Figure 1. Each separate dc source (SDCS) is connected to a single-phase H-bridge, inverter. Each inverter level can generate three different voltage outputs, $+V_{dc}$, 0, and $-V_{dc}$ by connecting the dc source to the ac output by different combinations of the four switches,

$$V_{AN} = V_{dc1} + V_{dc2} + \dots + V_{dc(S-1)} + V_{dcS} \quad (1.1)$$

S_1 , S_2 , S_3 , and S_4 . To obtain $+V_{dc}$, switches S_1 and S_4 are turned on, whereas $-V_{dc}$ can be obtained by turning on switches S_2 and S_3 . By turning on S_1 and S_2 or S_3 and S_4 , the output voltage is 0. The ac outputs of each of the different full-bridge inverter levels are connected in series such that the synthesized voltage waveform is the sum of the inverter outputs. The number of output phase voltage levels m in a cascade inverter is defined by

$$m = 2s + 1,$$

Where 's' is the number of separate dc sources.

An example phase voltage waveform for an m-level cascaded H-bridge inverter with S-SDCSs and S full bridges is shown in Figure 2

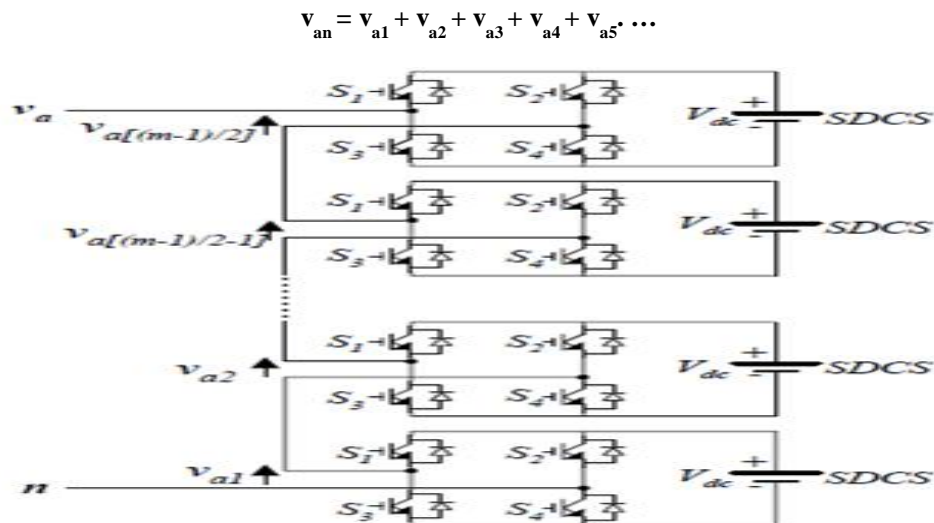


Fig. 2 Single-phase structure of a m level multilevel cascaded H-bridges inverter

International Journal of Advanced Research in Electrical, Electronics and Instrumentation Engineering

(An ISO 3297: 2007 Certified Organization)

Vol. 3, Issue 11, November 2014

II. CONVENTIONAL MULTYLEVEL H- BRIDGE TOPOLOGY

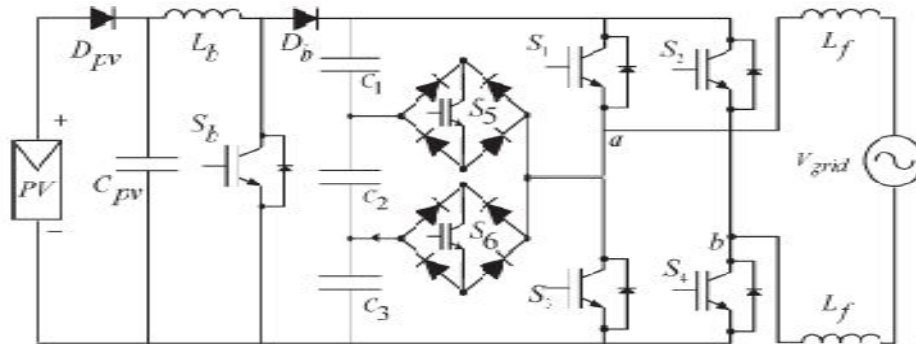


Fig.3 Proposed single-phase seven-level grid-connected inverter for photovoltaic systems.

The proposed single-phase seven-level inverter was developed from the five-level inverter. It comprises a single-phase conventional H-bridge inverter, two bidirectional switches, and a capacitor voltage divider formed by C_1 , C_2 , and C_3 , as shown in Fig. 3. The modified H-bridge topology is significantly advantageous over other topologies, i.e., less power switch, power diodes, and less capacitors for inverters of the same number of levels. Photovoltaic (PV) arrays were connected to the inverter via a dc–dc boost converter. The power generated by the inverter is to be delivered to the power network, so the utility grid, rather than a load, was used. The dc–dc boost converter was required because the PV arrays had a voltage that was lower than the grid voltage. High dc bus voltages are necessary to ensure that power flows from the PV arrays to the grid. A filtering inductance L_f was used to filter the current injected into the grid. Proper switching of the inverter can produce seven output-voltage levels (V_{dc} , $2V_{dc}/3$, $V_{dc}/3$, 0 , $-V_{dc}$, $-2V_{dc}/3$, $-V_{dc}/3$) from the dc supply voltage. The proposed inverter's operation can be divided into seven switching states, as shown in Fig. 4(a)–(g). Fig. 4(a), (d), and (g) shows a conventional inverter's operational states in sequence, while Fig. 4(b), (c), (e), and (f) shows additional states in the proposed inverter synthesizing one- and two-third levels of the dc-bus voltage. The required seven levels of output voltage were generated as follows.

- 1) Maximum positive output (V_{dc}): S_1 is ON, connecting the load positive terminal to V_d , and S_4 is ON, connecting the load negative terminal to ground. All other controlled switches are OFF; the voltage applied to the load terminals is V_{dc} . Fig. 4(a) shows the current paths that are active at this stage.
- 2) Two-third positive output ($2V_{dc}/3$): The bidirectional switch S_5 is ON, connecting the load positive terminal and S_4 is ON, connecting the load negative terminal to ground. All other controlled switches are OFF; the voltage applied to the load terminals is $2V_{dc}/3$. Fig. 4(b) shows the current paths that are active at this stage.
- 3) One-third positive output ($V_{dc}/3$): The bidirectional switch S_6 is ON, connecting the load positive terminal, and S_4 is ON, connecting the load negative terminal to ground. All other controlled switches are OFF; the voltage applied to the load terminals is $V_{dc}/3$. Fig. 4(c) shows the current paths that are active at this stage.
- 4) Zero output: This level can be produced by two switching combinations; switches S_3 and S_4 are ON, or S_1 and S_2 are ON, and all other controlled switches are OFF; terminal ab is a short circuit, and the voltage applied to the load terminals is zero. Fig. 4(d) shows the current paths that are active at this stage.
- 5) One-third negative output ($-V_{dc}/3$): The bidirectional switch S_5 is ON, connecting the load positive terminal, and S_2 is ON, connecting the load negative terminal to V_{dc} . All other controlled switches are OFF; the voltage applied to the load terminals is $-V_{dc}/3$. Fig. 4(e) shows the current paths that are active at this stage.

International Journal of Advanced Research in Electrical, Electronics and Instrumentation Engineering

(An ISO 3297: 2007 Certified Organization)

Vol. 3, Issue 11, November 2014

6) Two-third negative output ($-2V_{dc}/3$): The bidirectional switch S_6 is ON, connecting the load positive terminal, and S_2 is ON, connecting the load negative terminal to ground. All other controlled switches are OFF; the voltage applied to the load terminals is $-2V_{dc}/3$. Fig. 4(f) shows the current paths that are active at this stage.

7) Maximum negative output ($-V_{dc}$): S_2 is ON, connecting the load negative terminal to V_{dc} , and S_3 is ON, connecting the load positive terminal to ground. All other controlled switches are OFF; the voltage applied to the load terminals is $-V_{dc}$. Fig. 4(g) shows the current paths that are active at this stage.

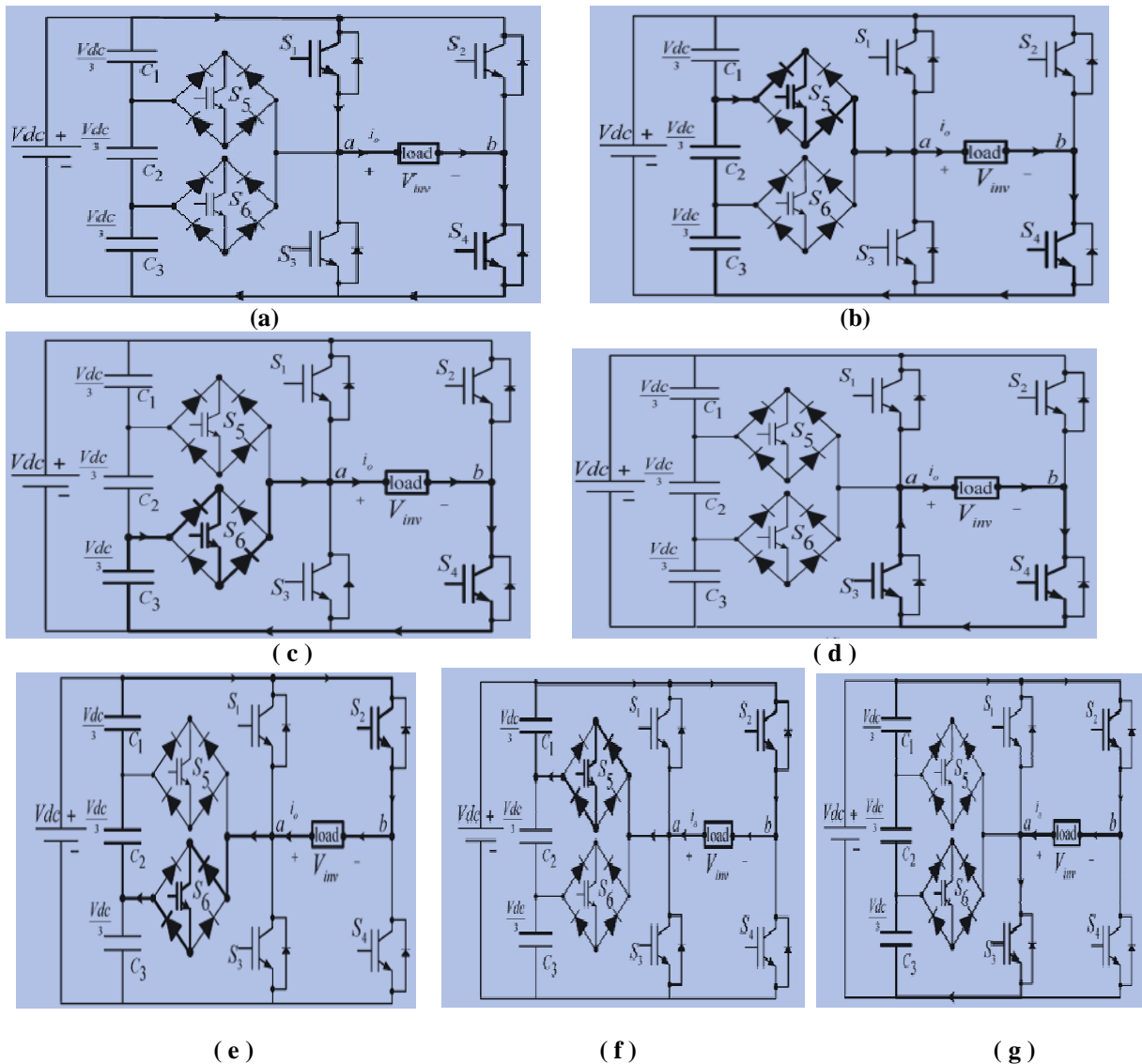


Fig. 4. Switching combination required to generate the output voltage (V_{ab}).

(a) $V_{ab} = V_{dc}$. (b) $V_{ab} = 2V_{dc}/3$. (c) $V_{ab} = V_{dc}/3$. (d) $V_{ab} = 0$. (e) $V_{ab} = -V_{dc}/3$. (f) $V_{ab} = -2V_{dc}/3$. (g) $V_{ab} = -V_{dc}$.



International Journal of Advanced Research in Electrical, Electronics and Instrumentation Engineering

(An ISO 3297: 2007 Certified Organization)

Vol. 3, Issue 11, November 2014

TABLE 1
Output Voltages According To Switches On-Off Condition

v_0	S_1	S_2	S_3	S_4	S_5	S_6
V_{dc}	on	off	off	on	off	off
$2V_{dc}/3$	off	off	off	on	on	off
$V_{dc}/3$	off	off	off	on	off	on
0	off	off	on	on	off	off
0^*	on	on	off	off	off	off
$-V_{dc}/3$	off	on	off	off	on	off
$-2V_{dc}/3$	off	on	off	off	off	on
$-V_{dc}$	off	on	on	off	off	off

Table I shows the switching combinations required to generate out put voltage.

2.1 PWM Modulation

A novel PWM modulation technique was introduced to generate the PWM switching signals. Three reference signals (V_{ref1} , V_{ref2} , and V_{ref3}) were compared with a carrier signal ($V_{carrier}$). The reference signals had the same frequency and amplitude and were in phase with an offset value that was equivalent to the amplitude of the carrier signal. The reference signals were each compared with the carrier signal. If V_{ref1} had exceeded the peak amplitude of $V_{carrier}$, V_{ref2} was compared with $V_{carrier}$ until it had exceeded the peak amplitude of $V_{carrier}$. Then, onward, V_{ref3} would take charge and would be compared with $V_{carrier}$ until it reached zero. Once V_{ref3} had reached zero, V_{ref2} would be compared until it reached zero. Then, onward, V_{ref1} would be compared with $V_{carrier}$. Fig. 3 shows the resulting switching pattern. Switches S_1 , S_3 , S_5 , and S_6 would be switching at the rate of the carrier signal frequency, whereas S_2 and S_4 would operate at a frequency that was equivalent to the fundamental frequency.

The phase angle depends on modulation index Ma . Theoretically for a single reference signal and a single carrier signal, the modulation index is defined to be

$$Ma = Am/Ac \quad (02)$$

while for a single-reference signal and a dual carrier signal, the modulation index is defined to be

$$Ma = Am/2Ac. \quad (03)$$

Since the proposed seven-level PWM inverter utilizes three carrier signals, the modulation index is defined to be

$$Ma = Am/3Ac \quad (04)$$

where Ac is the peak-to-peak value of the carrier signal and Am is the peak value of the voltage reference signal V_{ref} . When the modulation index is less than 0.33, the phase angle displacement is

$$\theta_1 = \theta_2 = \theta_3 = \theta_4 = \pi/2 \quad (05)$$

$$\theta_5 = \theta_6 = \theta_7 = \theta_8 = 3\pi/2. \quad (06)$$

International Journal of Advanced Research in Electrical, Electronics and Instrumentation Engineering

(An ISO 3297: 2007 Certified Organization)

Vol. 3, Issue 11, November 2014

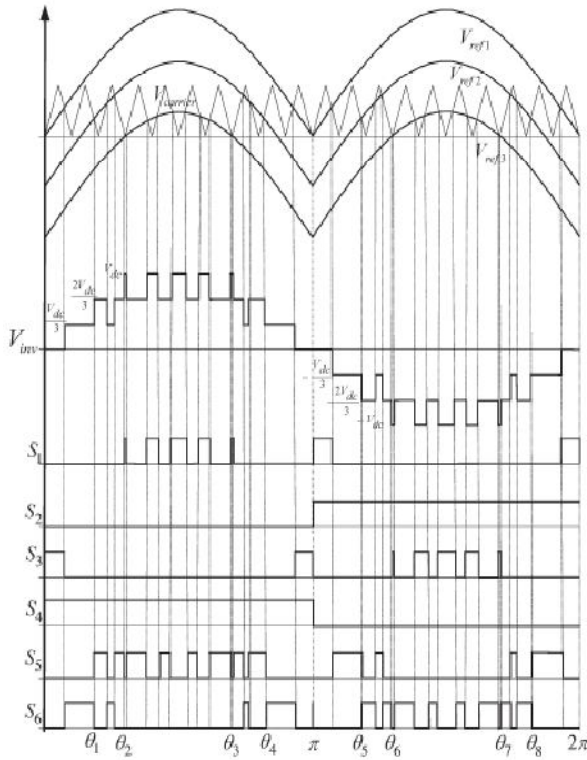


Fig. 5. Switching pattern for the single-phase seven-level inverter

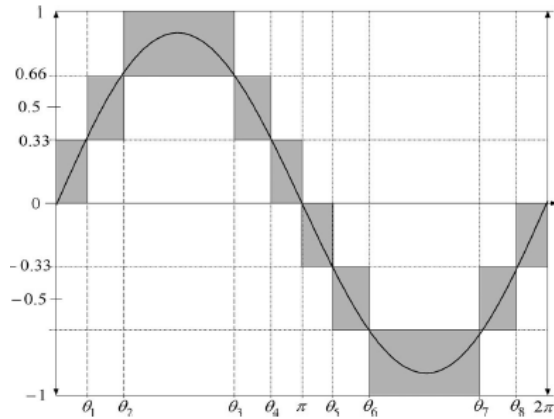


Fig. 6. Seven-level output voltage (Vab) and switching angles.

For one cycle of the fundamental frequency, the proposed inverter operated through six modes. Fig. 6 shows the per unit output-voltage signal for one cycle. The six modes are described as follows:

- Mode 1 : $0 < \omega t < \theta_1$ and $\theta_4 < \omega t < \pi$
- Mode 2 : $\theta_1 < \omega t < \theta_2$ and $\theta_3 < \omega t < \theta_4$
- Mode 3 : $\theta_2 < \omega t < \theta_3$
- Mode 4 : $\pi < \omega t < \theta_5$ and $\theta_8 < \omega t < 2\pi$
- Mode 5 : $\theta_5 < \omega t < \theta_6$ and $\theta_7 < \omega t < \theta_8$
- Mode 6 : $\theta_6 < \omega t < \theta_7$.

On the other hand, when the modulation index is more than 0.33 and less than 0.66, the phase angle displacement is determined by

$$\begin{aligned} \theta_1 &= \sin^{-1}(Ac/Am) & (07) \\ \theta_2 &= \theta_3 = \pi/2 & (08) \\ \theta_4 &= \pi - \theta_1 & (09) \\ \theta_5 &= \pi + \theta_1 & (10) \\ \theta_6 &= \theta_7 = 3\pi/2 & (11) \\ \theta_8 &= 2\pi - \theta_1. & (12) \end{aligned}$$

If the modulation index is more than 0.66, the phase angle displacement is determined by

$$\begin{aligned} \theta_1 &= \sin^{-1}(Ac/Am) & (13) \\ \theta_2 &= \sin^{-1}(2Ac/Am) & (14) \\ \theta_3 &= \pi - \theta_2 & (15) \\ \theta_4 &= \pi - \theta_1 & (16) \\ \theta_5 &= \pi + \theta_1 & (17) \\ \theta_6 &= \pi + \theta_2 & (18) \\ \theta_7 &= 2\pi - \theta_2 & (19) \\ \theta_8 &= 2\pi - \theta_1. & (20) \end{aligned}$$

For Ma that is equal to, or less than, 0.33, only the lower reference wave (Vref3) is compared with the triangular carrier signal. The inverter's behavior is similar to that of a conventional full-bridge three-level PWM inverter. However, if Ma is more than 0.33 and less than 0.66, only Vref2 and Vref3 reference signals are compared with the triangular carrier

International Journal of Advanced Research in Electrical, Electronics and Instrumentation Engineering

(An ISO 3297: 2007 Certified Organization)

Vol. 3, Issue 11, November 2014

3.3) Proposed FUZZY controller Circuit

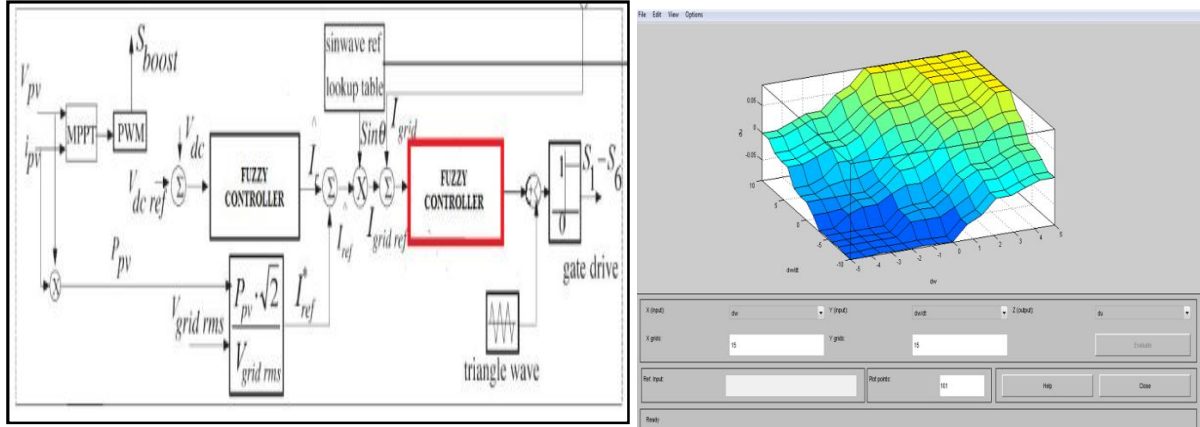


Fig. 8 Surface view of FIS editor

VI. COMPARISON of MATLAB /SIMULATION RESULTS

MATLAB SIMULINK simulated the proposed configuration before it was physically implemented in a prototype. The PWM switching patterns were generated by comparing three reference signals (V_{ref1} , V_{ref2} , and V_{ref3}) against a triangular carrier signal (see Fig. 6).

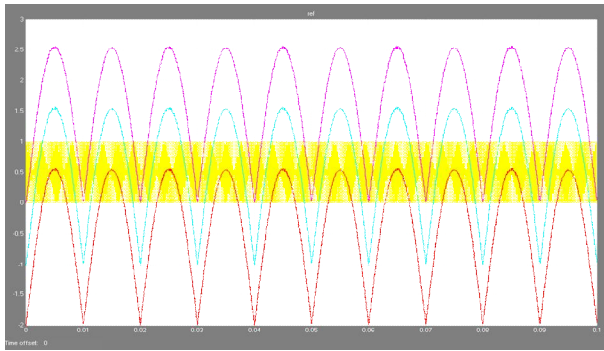


Fig. 6. PWM switching signal generation.

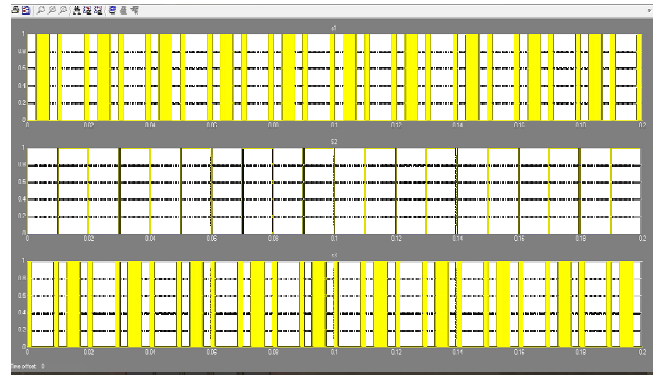


Fig. 7. Switching voltages of s1,s2 and s3

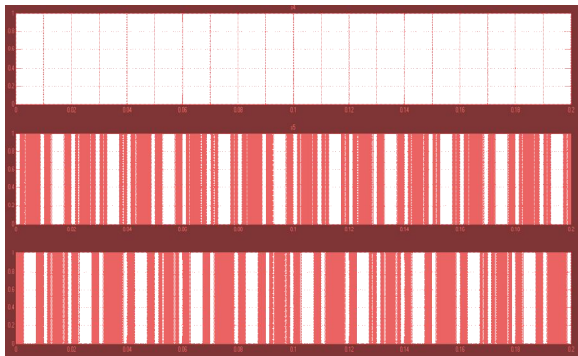


Fig.8. Switching voltages of s4,s5 and s6.

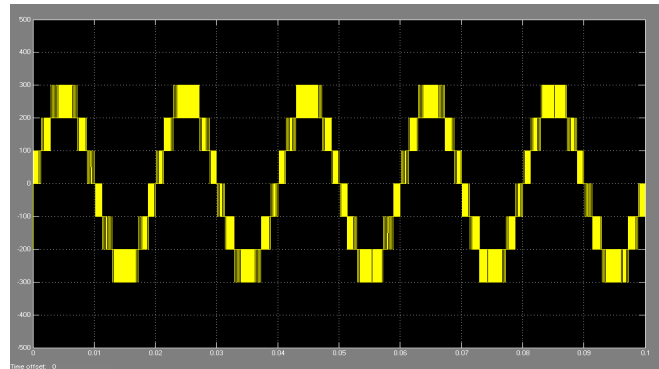


Fig. 9. conventional controller Inverter output voltage (V_{inv}).

International Journal of Advanced Research in Electrical, Electronics and Instrumentation Engineering

(An ISO 3297: 2007 Certified Organization)

Vol. 3, Issue 11, November 2014

Subsequently, the comparing process produced PWM switching signals for switches $S1-S6$, as Figs. 7–9 show. One leg of the inverter operated at a high switching rate that was equivalent to the frequency of the carrier signal, while the other leg operated at the rate of the fundamental frequency (i.e., 50 Hz). Switches $S5$ and $S6$ also operated at the rate of the carrier signal. Fig. 10. Inverter output voltage (V_{inv}). Fig. 11. Grid voltage (V_{grid}) and grid current (I_{grid}), of the carrier signal. Fig. 10 shows the simulation result of inverter output voltage V_{inv} . The dc-bus voltage was set at 300 V ($> \sqrt{2}V_{grid}$; in this case, V_{grid} was 120 V). The dc-bus voltage must always be higher than $\sqrt{2}$ of V_{grid} to inject current into the grid, or current will be injected from the grid into the inverter. Therefore, operation is recommended to be between $Ma = 0.66$ and $Ma = 1.0$. V_{inv} comprises seven voltage levels, namely, V_{dc} , $2V_{dc}/3$, $V_{dc}/3$, 0 , $-V_{dc}$, $-2V_{dc}/3$, and $-V_{dc}/3$. The current flowing into the grid was filtered to resemble a pure sine wave in phase with the grid voltage see Fig. 11). As I_{grid} is almost a pure sine wave at unity power factor, the total harmonic distortion (THD) can be reduced compared with the THD.

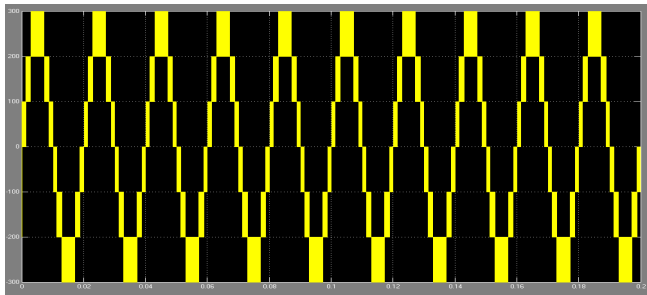


Fig.10. Proposed inverter out put voltage (V_{inv}).

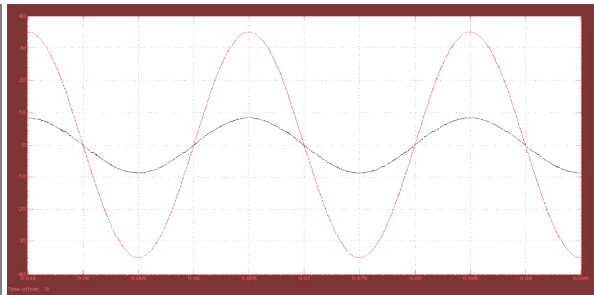


Fig. 11. Grid voltage (V_{grid}) and grid current (I_{grid}).

V. MULTILEVEL INVERTER SPECIFICATIONS AND CONTROLLER PARAMETERS.

The below table depicts the specifications and parameters of the inverter

TABLE - II

PV array rated voltage	1.2 kV
Standard Environmental Condition solar radiation	1000 W/m ²
Cell temperature, T	25 0 ^c
System Frequency	50 Hz
Switching Frequency	2K Hz
L_b	2.2mh
L_f	3mh
C1-C3	220 μ F
Inverter output voltage	300v

VI. CONCLUSION

7 level Multilevel inverters offer improved output waveforms and lower THD. This paper has presented a novel PWM switching scheme for the proposed multilevel inverter. It utilizes three reference signals and a triangular carrier signal to generate PWM switching signals. The behavior of the proposed multilevel inverter was analyzed in detail. A FUZZY control is implemented to optimize the performance of the inverter. By controlling the modulation index, the desired number of levels of the inverter's output voltage can be achieved. The less THD in the seven-level inverter compared with that in the five- and three-level inverters is an attractive solution for grid-connected PV inverters.

REFERENCES

[1] M. Calais and V. G. Agelidis, "Multilevel converters for single-phase grid connected photovoltaic systems—An overview," in *Proc. IEEE Int. Symp. Ind. Electron.*, 1998, vol. 1, pp. 224–229.



International Journal of Advanced Research in Electrical, Electronics and Instrumentation Engineering

(An ISO 3297: 2007 Certified Organization)

Vol. 3, Issue 11, November 2014

- [2] S. B. Kjaer, J. K. Pedersen, and F. Blaabjerg, "A review of single-phase grid connected inverters for photovoltaic modules," *IEEE Trans. Ind. Appl.*, vol. 41, no. 5, pp. 1292–1306, Sep./Oct. 2005.
- [3] P. K. Hinga, T. Ohnishi, and T. Suzuki, "A new PWM inverter for photovoltaic power generation system," in *Conf. Rec. IEEE Power Electron. Spec. Conf.*, 1994, pp. 391–395.
- [4] Y. Cheng, C. Qian, M. L. Crow, S. Pekarek, and S. Atcitty, "A comparison of diode-clamped and cascaded multilevel converters for a STATCOM with energy storage," *IEEE Trans. Ind. Electron.*, vol. 53, no. 5, pp. 1512–1521, Oct. 2006.
- [5] M. Saeedifard, R. Iravani, and J. Pou, "A space vector modulation strategy for a back-to-back five-level HVDC converter system," *IEEE Trans. Ind. Electron.*, vol. 56, no. 2, pp. 452–466, Feb. 2009.
- [6] S. Alepuz, S. Busquets-Monge, J. Bordonau, J. A. M. Velasco, C. A. Silva, J. Pontt, and J. Rodríguez, "Control strategies based on symmetrical components for grid-connected converters under voltage dips," *IEEE Trans. Ind. Electron.*, vol. 56, no. 6, pp. 2162–2173, Jun. 2009.
- [7] J. Rodríguez, J. S. Lai, and F. Z. Peng, "Multilevel inverters: A survey of topologies, controls, and applications," *IEEE Trans. Ind. Electron.*, vol. 49, no. 4, pp. 724–738, Aug. 2002.
- [8] J. Rodríguez, S. Bernet, B. Wu, J. O. Pontt, and S. Kouro, "Multilevel voltage-source-converter topologies for industrial medium-voltage drives," *IEEE Trans. Ind. Electron.*, vol. 54, no. 6, pp. 2930–2945, Dec. 2007.
- [9] M. M. Renge and H. M. Suryawanshi, "Five-level diode clamped inverter to eliminate common mode voltage and reduce dv/dt in medium voltage rating induction motor drives," *IEEE Trans. Power Electron.*, vol. 23, no. 4, pp. 1598–1160, Jul. 2008.
- [10] E. Ozdemir, S. Ozdemir, and L. M. Tolbert, "Fundamental-frequency modulated six-level diode-clamped multilevel inverter for three-phase stand-alone photovoltaic system," *IEEE Trans. Ind. Electron.*, vol. 56, no. 11, pp. 4407–4415, Nov. 2009.
- [11] R. Stala, S. Pirog, M. Baszynski, A. Mondzik, A. Penczek, J. Czekonski, and S. Gasiorek, "Results of investigation of multicell converters with balancing circuit—Part I," *IEEE Trans. Ind. Electron.*, vol. 56, no. 7, pp. 2610–2619, Jul. 2009.
- [12] R. Stala, S. Pirog, M. Baszynski, A. Mondzik, A. Penczek, J. Czekonski, and S. Gasiorek, "Results of investigation of multicell converters with balancing circuit—Part II," *IEEE Trans. Ind. Electron.*, vol. 56, no. 7, pp. 2620–2628, Jul. 2009.
- [13] P. Lezana, R. Aguilera, and D. E. Quevedo, "Model predictive control of an asymmetric flying capacitor converter," *IEEE Trans. Ind. Electron.*, vol. 56, no. 6, pp. 1839–1846, Jun. 2009.
- [14] M. F. Escalante, J.-C. Vannier, and A. Arzandé, "Flying capacitor multilevel inverters and DTC motor drive applications," *IEEE Trans. Ind. Electron.*, vol. 49, no. 4, pp. 809–815, Aug. 2002.
- [15] A. Shukla, A. Ghosh, and A. Joshi, "Static shunt and series compensations of an SMIB system using flying capacitor multilevel inverter," *IEEE Trans. Power Del.*, vol. 20, no. 4, pp. 2613–2622, Oct. 2005.
- [16] J. Huang and K. A. Corzine, "Extended operation of flying capacitor multilevel inverter," *IEEE Trans. Power Electron.*, vol. 21, no. 1, pp. 140–147, Jan. 2006.
- [17] F. Z. Peng, "A generalized multilevel inverter topology with self voltage balancing," *IEEE Trans. Ind. Appl.*, vol. 37, no. 2, pp. 611–617, Mar./Apr. 2001.
- [18] E. Villanueva, P. Correa, J. Rodríguez, and M. Pacas, "Control of a singlephase cascaded H-bridge multilevel inverter for grid-connected photovoltaic systems," *IEEE Trans. Ind. Electron.*, vol. 56, no. 11, pp. 4399–4406, Nov. 2009.
- [19] K. A. Corzine, M. W. Wielebski, F. Z. Peng, and J. Wang, "Control of cascaded multilevel inverters," *IEEE Trans. Power Electron.*, vol. 19, no. 3, pp. 732–738, May 2004.